
MEMORANDUM

NGST

Project Office

9 November 1998

Implications of the Mid-Infrared capability for NGST

P. Bély, R. Burg, S. Castles, M. Greenhouse, D. Jacobson,
K. Parrish, C. Perrygo, L. Petro, and D. Redding

Abstract

We compare the performance, cost and risk of three candidate NGST architectures: near-infrared optimized; mid-infrared compatible; and mid-infrared optimized. We conclude that the mid-infrared compatible concept, with optics and instrument modules passively cooled to about 40 and 30 K respectively is the most advantageous solution for NGST, whether mid-infrared instrumentation is added or not. Such a solution is not significantly more costly and offers lower risk because of the opportunity to passively cool the NIR detectors. This approach enables the mid-infrared, zodiacal light limited to 10 μm , without increasing complexity, risk or cost of the observatory. We recommend that the mid-infrared compatible architecture remain the basis for the continued NGST study.

1. Introduction

The core scientific mission identified by the "HST and Beyond" (Dressler) report [1] calls for a near-infrared (NIR) zodiacal light limited observatory working in the 1 to 5 μm range. Optimization of the observatory in that wavelength band has been interpreted as follows:

- diffraction limited imaging (Strehl of 0.8) at 2 μm ; and
- instrumental background in broadband (20%) imaging mode negligible compared to zodiacal light throughout the 1-5 μm band.

However, the Dressler report also advocates extending NGST's capability to the mid-infrared (MIR). This is interpreted as covering the 5 to 28 μm range (the Si:As detector practical range) with a sensitivity significantly better (e.g. >100 times) than that of the best existing or planned observatories in space (e.g. SIRTf) or on the ground (e.g. Keck). The arguments in the Dressler report are compelling and from the very beginning of the NGST study the 5-28 μm band was included as a stretch requirement [2].

NGST has many technical challenges, and it must be completed within a relatively tight schedule with a well-defined cost cap. All additions to NGST must be justified in terms of science return relative to risk and cost. This has led us to consider what is the relationship between cost and risk to the wavelength coverage. The Ad-hoc Science Working Group (ASWG) is presently assessing the science return for the relevant wavelength ranges. When the ASWG study is merged with the study being reported here, the arguments for or against inclusion of the extending the wavelength range of the NGST mission will be quantitatively understood.

In what follows we discuss our approach to optimization and then present reference architectures and compare them with respect to performance, risk and cost. We will often refer to the “Yardstick” architecture [3,4], a generic concept developed by the NGST Project Office to perform a broad range of analyses and serve as a reference design to which industry concepts can be compared [5,6]. The Yardstick concept, shown in Figure 1, uses only beryllium for the mirrors and supporting structure of the optical telescope assembly (OTA). Amongst all materials used in optical-mechanical systems, beryllium offers the best stiffness/mass ratio and a high conductivity leading to minimal temperature gradients in mirrors and supporting structures.

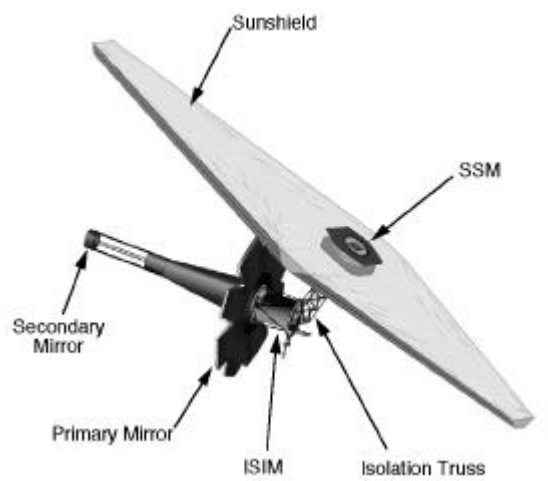


Figure 1. “Yardstick” architecture

2.0 Sensitivity considerations

2.1 Sources of backgrounds

NGST is being designed to significantly out-perform all existing and planned ground and space based observatories. The atmosphere and the relatively warm temperatures even on the highest mountains at night limit observations with ground telescopes in the infrared, even in the atmospheric windows. On the other hand, space-based MIR observatories to date, such as SIRTF, ISO and WIRE, are severely limited by the small aperture of their telescopes.

For a critically sampled diffraction-limited telescope, the sensitivity limit in the background-limited mode is given by:

$$S_{\text{lim}} = \frac{I \sigma}{D^2} \sqrt{\frac{B}{t}}$$

where σ is the desired signal-to-noise ratio, I the wavelength, D the diameter of the primary mirror, B the total background, and t the integration time. The background is composed of:

- zodiacal light;
- atmosphere emission (for ground based telescopes);
- detector dark current and readout noise;
- off-axis source straylight; and
- thermal self-emission from both the optics and from surrounding surfaces scattering off the optics.

Off-axis source straylight can be made negligible by proper baffling, so that for space telescopes the main sources of background are zodiacal light, thermal emission and detector noise. Thanks to its cryogenic optics and very low dark current detectors, SIRTf is zodiacal light limited for MIR imaging. With its 8-meter diameter, NGST offers a D^2 gain of 100 in signal strength over the 0.8 meter diameter SIRTf. But to be 100 times more sensitive (σ), NGST, like SIRTf, needs to be zodiacal light limited, and cannot suffer any loss due to detector noise or thermal self-emission from the optics. (In the spectroscopy mode, however, both observatories are detector noise limited and NGST will always be at least 100 times more sensitive.)

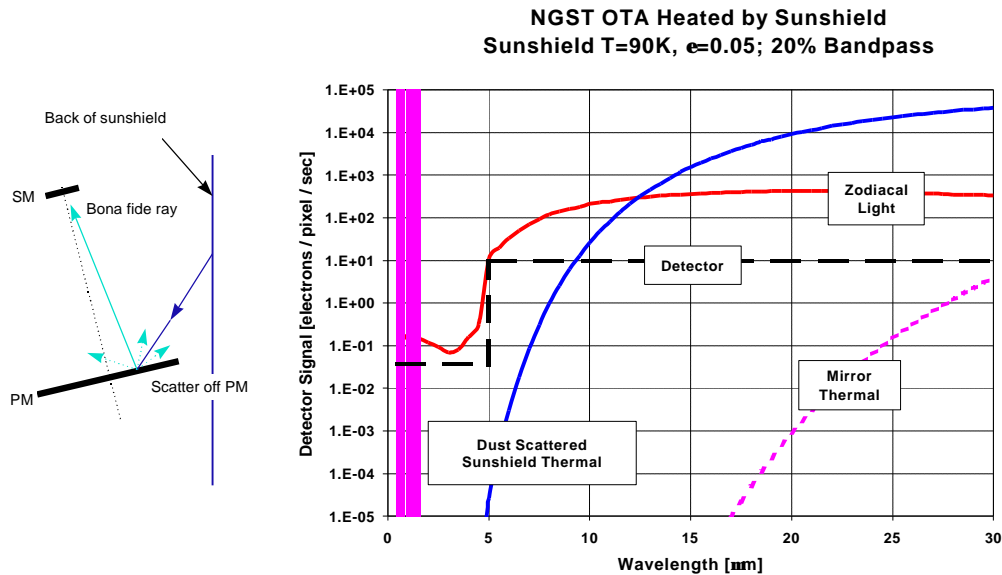


Figure 2. Scatter from the sunshield off the surfaces of the primary and secondary mirrors is the dominant source of thermal input at the focal plane (left). Typical fluxes due to the sunshield scatter and direct thermal emission of the mirrors are shown at right in the case of the Yardstick concept (reflective sunshield back layer at about 90 K).

All the architectures currently under consideration for NGST are designed as an “open tube” telescope behind a multi-layer sunshield. With the OTA’s large view to space, even a minimal sunshield allows the optics to cool to temperatures where their thermal emission is generally negligible compared to thermal emission from the sunshield scattering off the primary and secondary mirrors (Figure 2) [7].

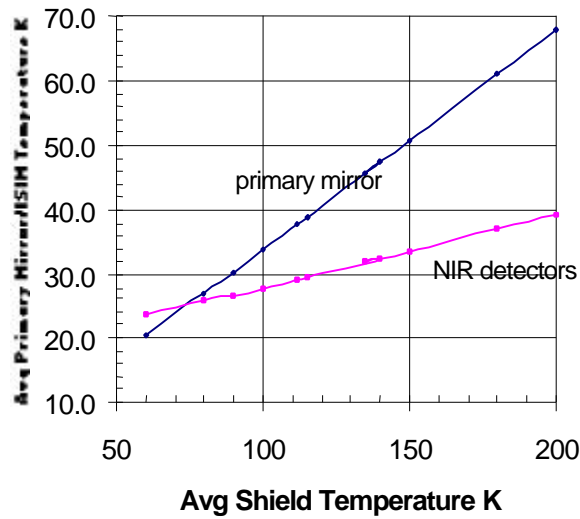


Figure 3. Temperature of the primary mirror and NIR detectors as a function of the temperature of the back layer of the sunshield. The calculations are based on the Yardstick configuration, assuming an emissivity of 0.05 for the sunshield and 0.03 for the mirror.

In our Yardstick concept studies, we found that a 90 K sunshield temperature appears feasible without undue risk and allows the NIR detectors to be passively cooled to their required temperature of 30 K (Figure 3) [3,8]. This corresponds to a zodiacal light background limit of about 12 μm (Figure 2). For NGST to be zodiacal light limited to 28 μm , the sunshield temperature needs to be approximately 50 K (Figure 4).

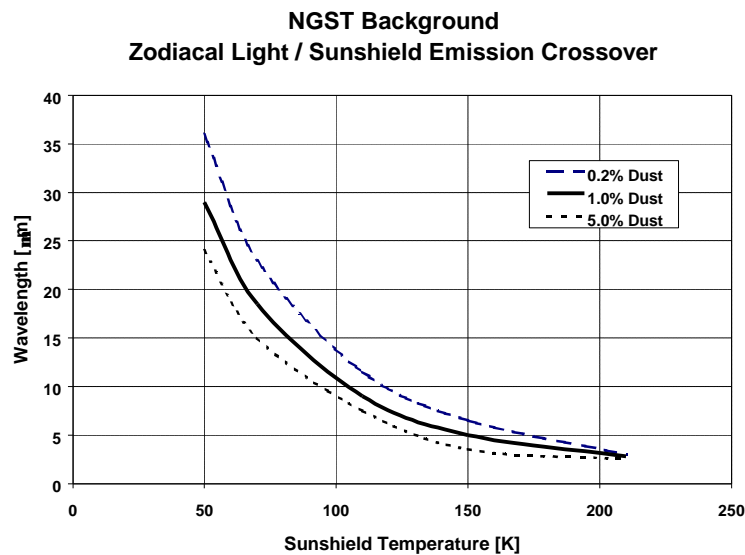


Figure 4. Wavelength at which the flux on the detector due to self-thermal emission of the purely passive observatory equals the flux of the zodiacal light for various levels of dust coverage on the optics (based on the Yardstick architecture).

2.2 Defining “Optimized” Architectures”

Based on the arguments developed above, NIR-optimization can be defined as the warmest optics and sunshield temperatures that yields zodiacal light limited performance up to $5\mu\text{m}$ wavelength. In practice, it is assumed that the “programmatic optimum” is obtained with optics at about 100 K; the practical temperature where the telescope can be tested using liquid nitrogen (LN2), thus reducing cost significantly. These two definitions are essentially the same: in the best case, 100 K optics (actively heated) combined with a cool enough sunshield will allow zodiacal limited observations up to $7\mu\text{m}$ (Figure 5).

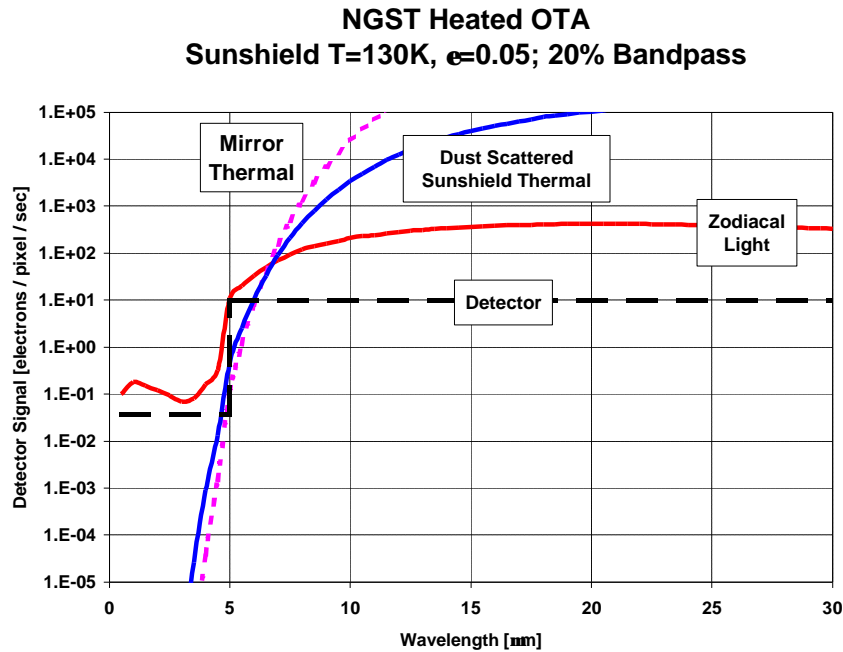


Figure 5. Flux at the focal plane from the optics, scatter from the sunshield and the zodiacal light in the case of the Yardstick-like architecture with a low emissivity sunshield at 130 K and optics actively heated to 100 K. The contributions of the optics and sunshield scatter are about equal. Such a system is zodiacal limited up to 7mm .

These considerations indicate that from the point of view of the wavelength coverage, NGST concepts fall into three categories:

1. “NIR-optimized”, where the telescope operating temperature is set at 100 K (zodiacal light limited to $7\mu\text{m}$) in the expectation that the fabrication and testing cost will be the lowest.
2. “MIR-compatible”, that is to say providing a respectable mid-infrared capability (zodiacal light limited to approximately $12\mu\text{m}$), but without pushing the technical aspects beyond what is required for NIR observations,

3. “MIR-optimized”, which is zodiacal light limited to 28 μm , clearly requiring a thermal design beyond what is necessary for NIR observations. “NIR-optimized”, where the telescope operating temperature is set at 100 K (zodiacal light limited to 7 μm) in the expectation that the fabrication and testing cost will be the lowest.

In what follows we first discuss the main design issues, then present reference architectures for the three options above and compare them from the points of view of performance, risk and cost.

3. Design issues

In this section we review the principal factors which affect the design, construction and operation of the observatory depending on its wavelength coverage.

3.1 Thermal stability

Compared to the well baffled and thermally controlled HST or to cryogenic telescopes such as ISO and SIRTF, NGST with its “open” telescope (no external baffle) is critically sensitive to the thermal environment; attitude changes will affect the alignment and figure of the optics. For a near infrared diffraction limited telescope, the relative position of most of the optical elements (e.g. the primary mirror segments) must not vary by more than about $5 \cdot 10^{-8}$ m ($\lambda/40$ on the mirror or a $\lambda/20$ wavefront error). Since the scale length of NGST is about a meter the allowable deformation is about 10^{-8} meter per meter. This means that either the coefficient of thermal expansion (CTE) of the structure and mirror material must be extremely low or the temperature field needs to remain, independent of attitude, constant to within approximately 0.1 K. (Or a combination of both of the above.) These are difficult requirements on the materials (Table 1) and therefore thermal stability issues are clearly at the heart of every NGST concept.

Table 1. Coefficient of thermal expansion at 40 and 100 K for various materials used in mirror blanks and telescope structures.

<i>Material</i>	<i>40 K</i>	<i>100 K</i>
Beryllium (O50)	$4 \cdot 10^{-8}$	$1.3 \cdot 10^{-6}$
Fused Silica	$0.6 \cdot 10^{-6}$	$-0.4 \cdot 10^{-6}$
Zerodur	$-6 \cdot 10^{-7}$	$-2 \cdot 10^{-7}$
Silicon carbide	$2 \cdot 10^{-7}$	$1 \cdot 10^{-7}$
Graphite Epoxy	10^{-7}	10^{-7}

One solution to the problem is to continuously control the position and figure of the optics using internal metrology and actuators. One possibility would be to use “edge sensors” between each of the mirror segments as in the Keck telescope [9], but this is not sufficient since the rest of the optical train is not monitored. A more complete solution is the “optical truss” [10] shown in Figure 6. Multiple laser beams are launched from around the secondary mirror in order to measure the position of the tertiary mirror and each segment of the primary mirror, allowing the position of the optics to be continuously corrected as the thermal or dynamics environment changes. Additional metrology can be used to measure and correct the figure of each of the segments. This is clearly a relatively complex and expensive solution, and reliability for a 5 to 10-year mission may be a problem.

Since the thermal environment at the L2 orbit is benign, and dynamics effects in a slow moving telescope observatory minimal, all the architectures currently proposed for NGST are “passive” and rely on thermal stability over long periods. But this requires that the optics stay aligned and the optical figure unchanged independently of the attitude of the telescope. The optics can be re-calibrated at periodic intervals to correct for drifts, but this should not occur more often than a few weeks apart so as not to significantly reduce observing efficiency. Thus, it is important that the OTA be thermally stable for extended periods of time.

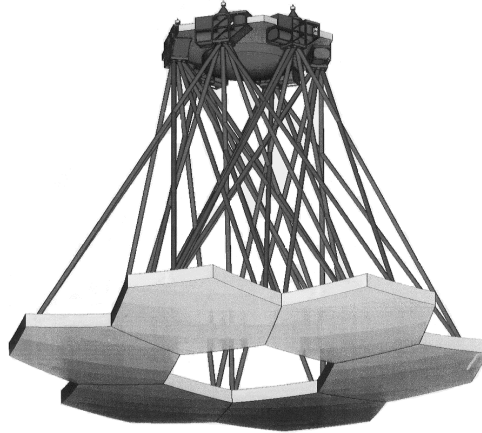


Figure 6. In the “optical truss” approach, continuous laser metrology and active control of each optical element of a telescope is used to maintain their precise respective position and figure independently of the thermal and dynamic disturbances. This solution is not currently considered for NGST because of its complexity and cost. The relatively benign dynamic and thermal environment of the L2 orbit favors a “passive” solution.

3.2 Sunshield geometry and OTA temperature field variation

At the L2 orbit, the dominant external disturbance force is due to solar pressure acting on the sunshield. This force is on the order of 1 N. The observatory must be designed such that the solar force vector passes close to the center-of-mass. If not, the reaction wheels used for attitude control will quickly saturate and require frequent thruster firings to unload their momentum. In the architectures currently proposed for NGST, the sunshield is extended below the OTA beyond what is geometrically required for shading in order to satisfy the center of pressure/center of mass condition. This results in a large sunshield. An alternate solution, which is potentially advantageous from the cost and dynamics points of view, would conform the shield to the OTA and use a solar trim sail to properly shift the center of pressure. In addition to providing a static shift in center of pressure, the solar trim sail could also be articulated to provide active control of solar torque and thereby greatly decrease the need for thruster firings to unload momentum (Figure 7).

However, a conformal or L-shaped sunshield adversely affects thermal stability of the OTA. Ignoring conduction within the OTA, the temperature of each element of the OTA is a function of that element’s view factor to the back side of the sunshield and the temperature of that portion of the sunshield that is viewed. Elements of the OTA located close to the sunshield are more tightly coupled radiatively to the sunshield than elements farther away. Consequently, these close elements are warmer and vary more in temperature with changes in sunshield temperature.

Changes in sunshield temperature occur when the observatory slews and changes its pitch angle with respect to the sun producing a change in the heat flux on the sunshield. A planar sunshield changes temperatures rather uniformly with pitch angle and maximum temperature changes on the back-side are just a few degrees. As a result, temperature changes in the OTA are only a couple of degrees at most. The better the thermal isolation performance of the sunshield then the smaller the change in OTA temperature with pitch angle. Figure 8 shows the transient temperature response of the yardstick design after a worst case slew of 27. An L-shaped sunshield is not nearly so well behaved. As illustrated in Figure 9, the primary mirror is strongly coupled radiatively to the foot portion of the L-shaped sunshield. Due to this geometry, the temperature distribution with the sunshield varies many tens of degrees with pitch angle.

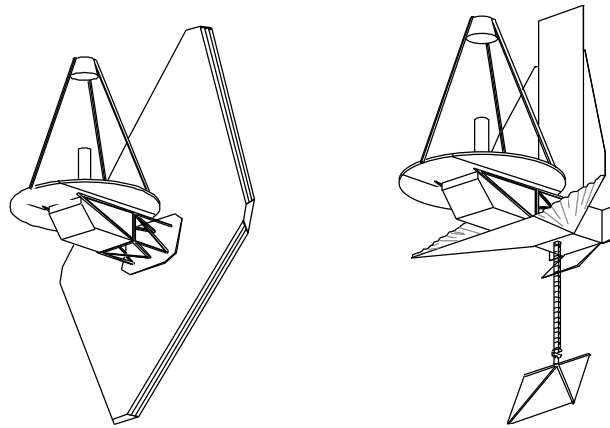


Figure 7. In Yardstick-like architectures, solar torque is minimized by extending the sunshield below the OTA (left). An alternate is to use a conformal sunshield with a solar sail to balance the solar torque (right).

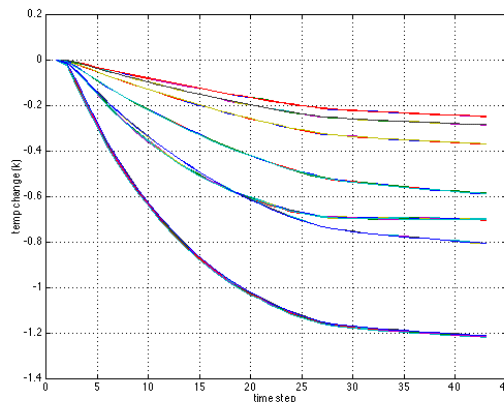


Figure 8. Temperature change of each of the 8 mirror petals of the Yardstick design following a 27° pitch slew (worst hot to cold case). The temperature of the leading petal (closest to the sunshield) varies by 1.2 K, while that of the aft petal (away from the sunshield) varies about 6 times less.

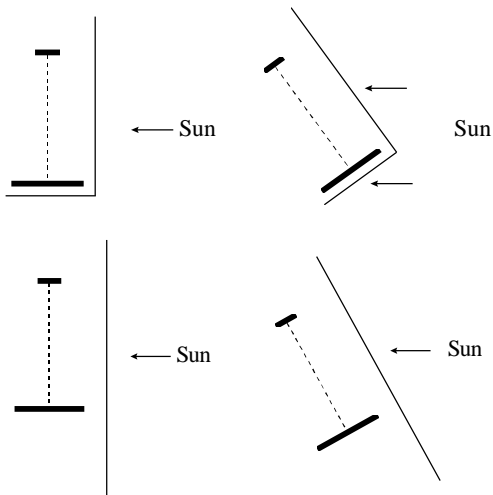


Figure 9. An attitude change in the L-shaped shield architecture (top) leads to drastic temperature changes whenever the back of the mirror is illuminated directly because of the close proximity of the primary mirror to the rear sunshield and because the heat input varies as a sine law. In the case of the planar sunshield (bottom), the thermal changes are much smaller because they follow a cosine law

3.3 Effect of a varying temperature field on image quality

As discussed earlier, the image quality of the optics is very sensitive to temperature variations. The Yardstick all-beryllium architecture, with a 40 K OTA, benefits from a material with high conductivity and low CTE and does not suffer from mixed materials effects. Still, a 27° slew in pitch degrades image quality to below the requirement. The effect of this worst case slew is shown in Figure 10. During the course of the day following such a slew, the wavefront error increases from 2 to $3.5 \cdot 10^{-7}$ m rms, and the Strehl decreases from a nominal value of 0.8, the “diffraction limit” according to the Maréchal condition, to 0.7.

However, most of the wavefront error comes from bulk deformation of the structure and to a lesser extent from radius of curvature changes, and not from figure degradation within the individual mirror segments. Although the average temperature of each mirror segment changes, gradients are extremely low (on the order of 0.01 K across a segment) so that their figures are unaffected except for a slight radius of curvature variation. Hence, image quality can be restored by adjustment of the mirror support points. This could be done with open loop mirror position correction following detailed calibration of the effects. Alternatively, a relatively simple thermal control can be used to maintain a constant (although not necessarily isothermal) temperature field.

This problem is exacerbated in architectures which suffer from larger OTA deformation either due to larger temperature variations or because the CTE of the material is higher. In these cases, more precise thermal control is required.

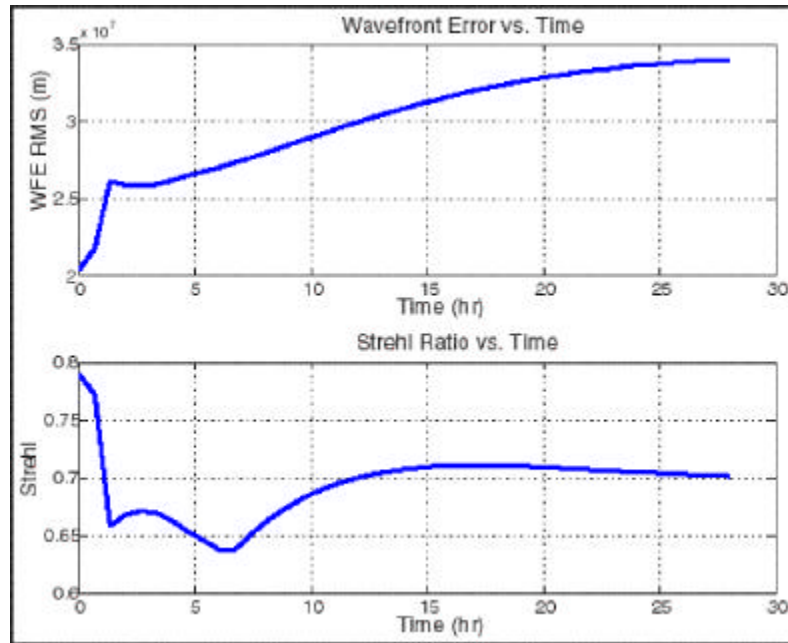


Figure 10. Effect of a worst case hot to cold slew on image quality in the case of the Yardstick architecture. The wavefront error is shown at the top (in 0.1m units) and in terms of the Strehl ratio at the bottom.

3.4 Is a “heated” OTA less sensitive to slews?

In the case where a high performance planar sunshield is used, heating the OTA to a temperature higher than the temperature obtained passively will significantly reduce the temperature change due to slews. This is because the energy balance of the OTA is now primarily a function of the heater input and radiation to space, with the heat from the sunshield radiation playing only a minor role. Figure 11 shows the variation in the mirror temperature due to slew as a function of the temperature to which it is actively raised using an open loop heater control. For a primary mirror heated to 100 K, the variation in temperature variation due to a maximum slew (27° in pitch) is on the order of 0.1 K; a variation about 10 times less than what it is at 40 K. However, the actual deformation of a beryllium mirror (mirror and supporting structure) will actually be higher because the CTE of beryllium at 100 K is about 25 times larger than at 40 K (Table1). Hence, in the case of the all-beryllium Yardstick, open loop heating the OTA will not improve dimensional stability because of the extremely low CTE of beryllium at 40 K. Other materials, especially those with CTE that varies weakly with temperature do benefit from this technique.

3.5 Sunshield design

Thermal isolation performance of the sunshield is dependent upon the number of reflective film layers in the sunshield, and the separation between those layers. By separating film layers, isolation performance is greatly improved for two reasons. First, conductance between layers is reduced to zero except at physical attachment points to the shield layers. In the yardstick planar sunshield concept, the film layers are supported only at the tips of the deployment booms and at their attachment to the spacecraft support module (SSM). These attachment points utilize low-conductance materials to minimize conductive heat transfer between shield layers.

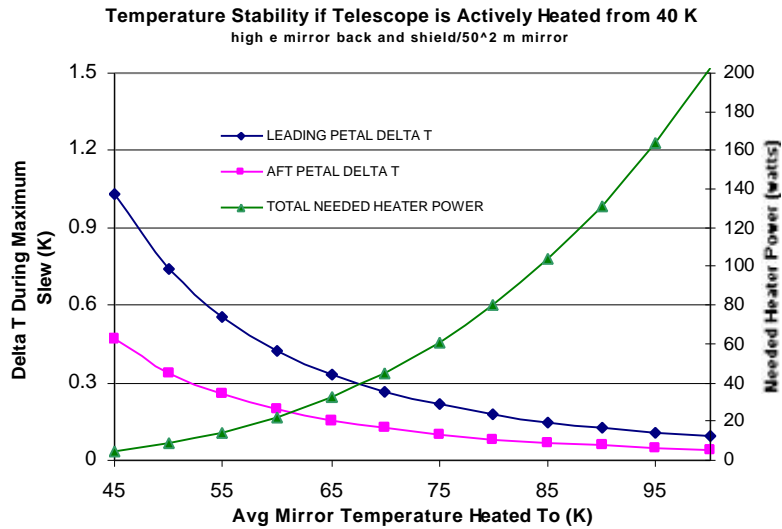
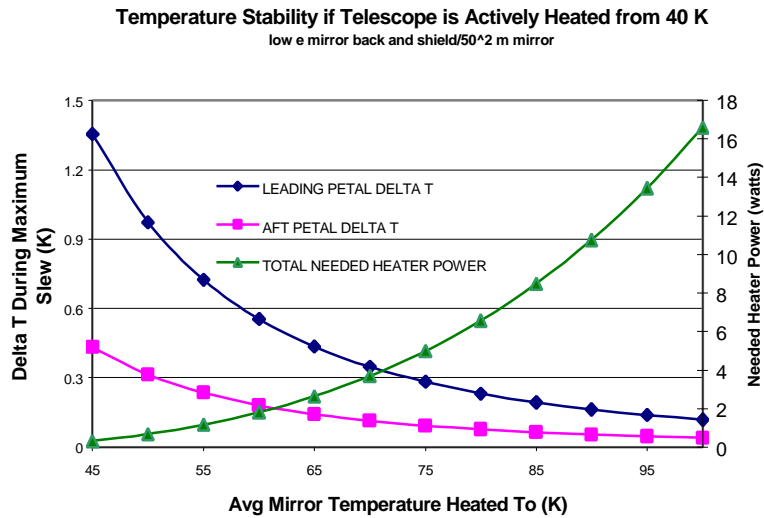


Figure 11. Changes in the temperature of the aft and leading petal of the OTA following a 27° pitch as a function of the temperature to which the mirror is actively heated. Calculation is based on the Yardstick design with beryllium mirrors. The case of a low emissivity mirror back is shown at the top. The high back emissivity case is shown at the bottom. In both cases, the heating system is assumed to be open loop. Also shown is the heat input required to actively raise the temperature of the mirror above its passive temperature of 40 K (scale a right).

Second, the gap between the layers combined with the high reflectance of the film surfaces results in much of the internal radiant energy reflecting between two layers to escape to space. With a 97% reflectance, a typical photon is on the average reflected over twenty times before being absorbed. Thus, a gap between adjacent film layers allows photons to escape to space before being absorbed. Figure 12 shows the improvement provided by separating film layers compared to traditional multi-layer insulation (MLI) blankets. Cooling the OTA below 70 K using a sunshield consisting of an MLI blanket requires a large number of layers. At 5 to 10 kg

per layer for the film alone plus additional mass for structural support, the sunshield mass becomes excessive and the use of separated film layers is required.

While two layers provides adequate thermal isolation for a 100 K OTA, two layers are unacceptable from a straylight perspective. The sunshield will be pierced by a large number of micrometeoroids over its lifetime. With only two layers, there is a risk of unacceptably high straylight due to large holes and tears. Additional layers provide significant reduction in straylight. Three film layers generate unbalanced compressive tip forces on the sunshield deployment booms that reduce the strength of these booms. An even number of layers is required so as not to generate any bending moments on the booms, and therefore four layers is considered to be the minimum acceptable.

As the required OTA operating temperature is lowered, film separation and/or number of layers needs to increase to adequately reduce the heat load from the sunshield. Eight layers in the form of two four-layer sunshields, separated by approximately one-meter, will reduce the cold-side temperature of the sunshield to about 30 K. This will be adequate for the MIR-optimized architecture if conduction heat loads can also be reduced.

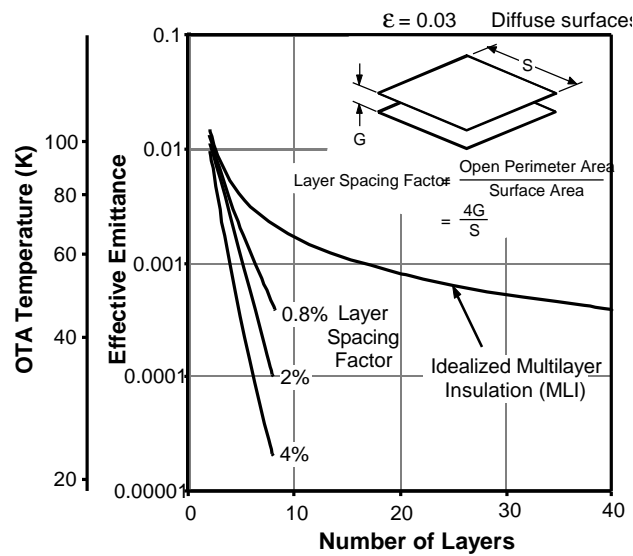


Figure 12. Sunshield performance and resulting OTA temperature (for yardstick planar sunshield configuration) as a function of layer number and spacing.

3.6 Detector cooling

The NIR detectors need to be cooled to about 30 K in order to reduce the dark current noise to an acceptable level [2]. If the nearby OTA is cold enough (e.g. 40 K), and heat leaks adequately reduced, then these detectors can be passively cooled, provided that heat dissipation within the instruments is low enough. The heat generated in the integrated science instrument module (ISIM) is dominated by the readout of the detectors, and is on the order of 200 mW. At about 30 K, a radiator has an emissive power of about 46 mW/m², so that a 4-m² radiator is sufficient provided that it is placed such that the view factors to the OTA and sunshield are low.

With a “warm” OTA (e.g. 100 K), passive cooling of the ISIM to 30 K becomes very difficult and active cooling is required. Given the high levels of heat generated by the NIR detectors, the use of stored cryogens in a ten-year mission is impractical. A mechanical cryo-cooler is the only possible solution.

Cooling the MIR detectors to 7 K by passive means is not feasible. Either a mechanical or a stored-cryogen cooler is required for all the considered architectures.

3.7 Actuators and mechanisms

There are four generic types of actuators under consideration for use in NGST; electromagnetic, piezoelectric, electrostrictive and magnetostrictive. Electromagnetic actuators are conventional motors using both permanent and electric magnets. The performance of this class of actuators remains roughly constant with temperature. Care must be taken in the types of lubricants used at low temperature and material selection and dimensions must take into account thermal contraction going from room temperature to very low temperatures. The other actuator types are of the form where a change in applied voltage or current changes the strain, and hence the shape, of the material. The change in shape is either used to directly produce the desired effect (as in the FSM) or configured in a device such as an inch-worm actuator to provide greater motion (mirror position actuators). Both piezoelectric and electrostrictive actuators are more efficient at high temperatures than at low temperatures while magnetostrictive materials are more efficient at low temperature than at high temperature. Actuators made from piezoelectric or electrostrictive materials, if sized for low temperature operation, are guaranteed to work for room temperature testing. For magnetostrictive actuators this is not the case. In conclusion, there does not seem to be strong technical or cost issues involved with actuators with respect to the operating temperature.

NGST has several mechanisms used for deployment and in instrument configuration changes. The actual deployment will be done warm and therefore there should not be a strong temperature dependence to the cost of developing or building these systems.

3.8 Testing Facilities

The basic testing philosophy adopted for NGST is well described in a Lockheed-Martin white paper [11]. Verification should be done *incrementally*, “whereby final observatory performance is verified by mathematical models, which are incrementally validated at the various subsystems levels”. This translates into a requirement for distributed testing facilities. The major tests that drive the costs for the NGST integration and test program are listed in Table 2 and require the following thermal test facilities:

- A. a medium-size chamber (~3-m diameter) for ISIM/Truss tests at the ISIM integrator facility;
- B. a medium-size chamber (~3-m diameter) for cryo-figuring of individual petals (if required by the mirror system), secondary and tertiary at the optics fabricator;
- C. a large-size chamber (>8-m diameter) at the optics fabricator for primary mirror/OTA level tests;
- D. a large-size chamber (>8-m diameter) at the systems integrator for final system tests;

- E. small cryostats to test individual components of the OTA (DM, FSM, isolation truss, and actuators) and of the science instruments (NIR camera and NIR spectrograph);
- F. and two small chambers to test the assembled NIR camera and the NIR spectrograph.

All of the above-listed chambers need only to be operated at LN2 temperatures (~100 K) for the NIR-optimized architecture. For both the MIR-compatible and MIR-optimized architectures, several but not necessarily all of these chambers need to be upgraded to Liquid Helium (LHe) capability (~40 K). Chambers A and B certainly require LHe temperatures for the MIR-compatible and the MIR-optimized architectures. The need for a final end-to-end LHe test is still under study and may depend on the specifics of the chosen architecture. As an example, the primary mirror and OTA verification test can be done at the higher temperature if the system is designed so that the residual figure errors combined with the dynamic range of the actuators result in analysis uncertainties at LHe temperatures that are small compared to the requirements. For the purpose of this study we have assumed that chamber D would need to be modified for a full final systems test at LHe temperatures.

Table 2. System level tests requiring cryogenic facilities

<i>Test</i>	<i>Chamber</i>
Component Tests	
1. FSM	E
2. DM	E
3. Mirror Actuators	E
4. Isolation Truss	E
Mirror/OTA tests	
5. Cryofiguring of primary mirror segments	B
6. Hindel test of secondary mirror for cryo-figuring	B
7. Cryo-figuring of tertiary mirror	B
8. PM verification	C
9. SM verification	B
10. TM verification	B
11. OTA verification	C
Instrument Tests	
12. NIR Camera	F
13. NIR Spectrograph	F
ISIM test	
14. ISIM/thermal truss thermal balance verification	A
15. ISIM verification	A
System tests	
16. Spacecraft/Truss thermal balance	D
17. Sunshield scale model test	D
18. OTA/ISIM verification	D

It has been suggested that chambers A and D would have to be LHe thermal-vacuum chambers whether the OTA was 100 K or 40 K since only with a very cold chamber can the appropriate thermal balance test be performed. This would then lower the cost difference between MIR-

compatible and NIR-optimized architectures considerably. It has also been suggested that if low temperature testing of all components is done early in the program (as indeed is the plan), then the risks due to low temperature are retired at those early incremental test stages. Thus the cost of upgrading the large chamber might not be needed. To be conservative, we have not adopted these two suggestions, but they will be studied in the future.

The existence of large and medium sized chambers with LN2 capabilities at Lockheed-Martin, ROSI, JSC, GSFC, MSFC, Ball Aerospace and at TRW that are suitable for NGST have been identified. The cost of upgrading these facilities has been estimated in section 5.1.

4. Reference architectures

NGST's requirements can be satisfied by a wide variety of architectures. In order to avoid confusing the comparison that we are after by introducing aspects that are unrelated to the thermal requirements, this analysis is based on a common architecture. Deviations from the yardstick-like design are taken only when warranted due to very different thermal conditions. In this section we present three reference architectures corresponding to the NIR-optimized, MIR-compatible, and MIR-optimized cases that we defined at the end of section 2. These architectures are essentially based on the Yardstick except that we adopted the fixed isolation truss and primary mirror chord fold approach developed by Ball Aerospace [6].

4.1 NIR-optimized architecture with 100 K OTA

In the NIR-optimized solution, we assume that the OTA is at 100 K in order to save on the integration and testing (LN2 instead of LHe). This can be obtained either by passively heating the OTA with a "warm sunshade" or by using a high performance sunshield and heating the OTA with auxiliary heaters to the target temperature. Figure 13 shows the three architectures that we have considered. In the NIR-1 and NIR-2 schemes, the sunshields are relatively inefficient in order to provide most of the heat required to maintain the OTA at 100 K. The NIR-3 scheme uses a more efficient sunshield which can passively cool the OTA to 40 K, but includes an OTA thermal control system to heat the OTA to 100 K.

In earlier comparisons of the NIR and MIR optimized NGST, for simplicity, we had used the same overall architecture and determined the cost difference due to the different operating temperatures [5,6,12]. The potential flaw in this approach is that there is no reason for a given architecture to remain "optimized" when the environmental conditions are significantly different. NIR-1 is an attempt to develop a design specifically for 100 K operation. Because of the higher operating temperature, it is possible to locate the sunshield close to the OTA/ISIM. This leads to a much more compact observatory. The sunshield is sized to protect the OTA side, and the back of the primary mirror has its own insulation. The sunshield is composed of a rigid frame supporting MLI insulation. For stowage, the sunshield stows over the folded primary mirror providing contamination protection. The non-symmetrical sunshield, however, creates an unacceptable overturning moment due to the long lever arm between the center of pressure and the center of gravity. As described in the previous section, a solar sail mounted on a long deployable boom attached to the SSM balances the solar torque and dumps excess momentum.

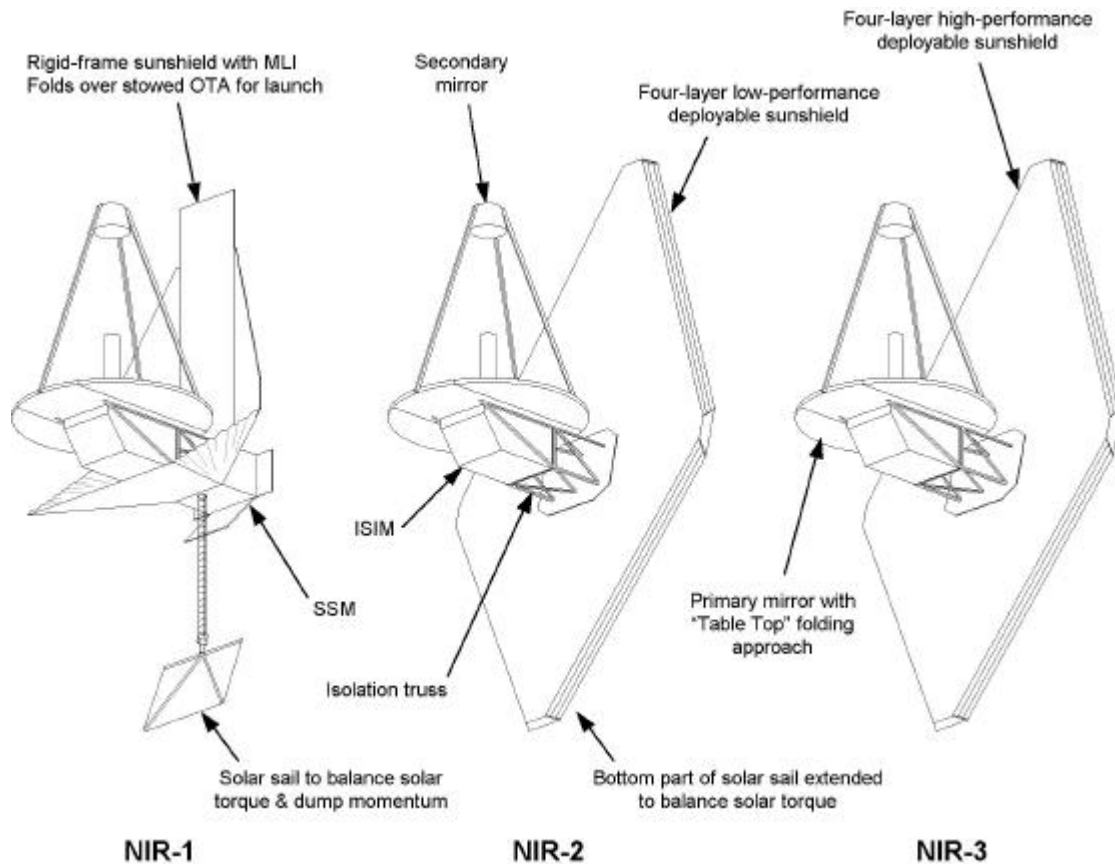


Figure 13. The three NIR-optimized architectures that we have considered. NIR-3 is essentially the yardstick architecture. NIR-2 is similar except that its sunshade is less efficient in order to heat up the OTA to about 100 K. NIR-1 is an attempt at tailoring the configuration to the “warm” OTA condition in order to reduce cost.

The advantages of such a compact design are multiple:

- the sunshield is smaller, potentially reducing its development cost and risk;
- the overall observatory structure is stiffer, adding robustness to the attitude control and vibration isolation system; and
- the overall observatory is lighter giving additional launch margin.

As shown in section 3.2, the main disadvantage of this design is that the primary mirror needs a precise, high dynamic range, active thermal control system because of the unfavorable L-shape of the sunshield. Our thermal analysis of this configuration indicates that without active control, the primary mirror average temperature would vary from 100 K in the hot case (0° pitch) to 60 K in the cold case (27° pitch). This large dynamic range puts an enormous strain on the mirror thermal control is thus considered impractical.

NIR-2 avoids the large temperature swing problem of NIR-1 by using a large, flat, sunshield like the one of the Yardstick architecture, albeit with a lower efficiency (effective emissivity of 0.021) in order for the OTA to passively reach a temperature close to 100 K. Heaters are then utilized to make the OTA isothermal for the entire attitude range of observatory. Table 3 gives the relevant thermal data for this solution. As expected the temperature variation without active

control is much smaller (3 to 4 K), which makes the task of the thermal control system easier, and only 3 Watts would be required to maintain temperature stability of the mirror. However, a closed loop heater system will be required to sense temperatures throughout the OTA and deliver proportionally controlled heater power making this solution somewhat complicated and unattractive.

Table 3. Thermal data for the NIR-2 solution

	0° pointing	27° pointing	ΔT during slew
Number of sunshield layers	4		
Sunshield effective emissivity	0.011		
Sunshield temperature (K)	140.0	135.0	-5.0
Primary mirror temperature			
Average (K)	104.3	100.6	-3.75
Aft petal (K)	118.8	114.5	-4.3
Leading petal (K)	89.9	86.7	-3.2
Petal ΔT (K)	28.9	27.8	-1.4
Power needed to isothermalize (W)	11.4	9.8	
Power needed to maintain temperature stability (W)		3.0	

NIR-3 utilizes a high performance sunshield (effective emissivity of 0.00021) that cools the OTA to about 40 K (as in the Yardstick architecture) and then has a relatively simple open loop heating system (stable to 0.1%) to raise the average OTA temperature to 100 K. At 100 K, the energy balance within the OTA is high enough to render the OTA relatively insensitive to the shield temperature variations due to observatory slews. The result is a very stable OTA with less than a 0.06 K shift after a worst-case slew (Table 4).

As explained in sections 3.2 and 3.3, NIR-1 and -2 thermal systems are more complex than that of NIR-3. As for mechanical systems, the NIR-1 sunshield did not turn out to be significantly different in cost. NIR-3 is the simplest of this class of options from the critical thermal control perspective and this is the one that we have kept for cost and risk analysis.

Table 4. NIR-3 Thermal data

	0° pointing	27° pointing	ΔT during slew
Number of sunshield layers	4		
Sunshield effective emissivity	0.00021		
Sunshield temperature (K)	115.0	111.3	-3.6
Primary mirror average temper. (K)	101.72	101.66	-0.06
Power needed to raise temperature to 100 K and isothermalize (W)	19.8	19.8	

4.3 MIR-compatible architecture

This case (Figure 14) is essentially that of the Yardstick concept and of the pre-Phase-A industry architectures that allows the NIR detectors to be passively cooled to 30 K. As shown in Figure 3 this requires a maximum sunshield temperature of 90 K. To provide this back-side temperature, the sunshield is composed of 6 layers separated by about 0.3-m (effective emissivity of 0.0001). This enables zodiacal light limited observations up to 12 μm (Figure 4). If no active thermal control is used, the OTA average temperature would vary by about 1 K and the maximum mirror

gradient would shift 0.2 K after a maximum observatory slew of 27° (Table 5). Modeling of the image quality indicated that the resulting image quality is borderline (Strehl of 0.7 after the slew, Figure 11). The image quality could be improved by frequent correction of the optics alignment during the thermal transient, but this requires significant time to slew to a suitably bright calibration star, acquire data, slew back, and perform the calculation. It is more efficient and relatively simple to use thermal control. Keeping the OTA completely isothermal requires only about 0.08 W. In practice, however, all that is required is that the OTA remain thermally stable. In that case, the active heating system only needs to deliver 19 mW over the OTA to maintain the pre-slew temperature field. This is a simple solution that utilizes the minimum amount of thermal control to guarantee a robust diffraction limited point spread function.

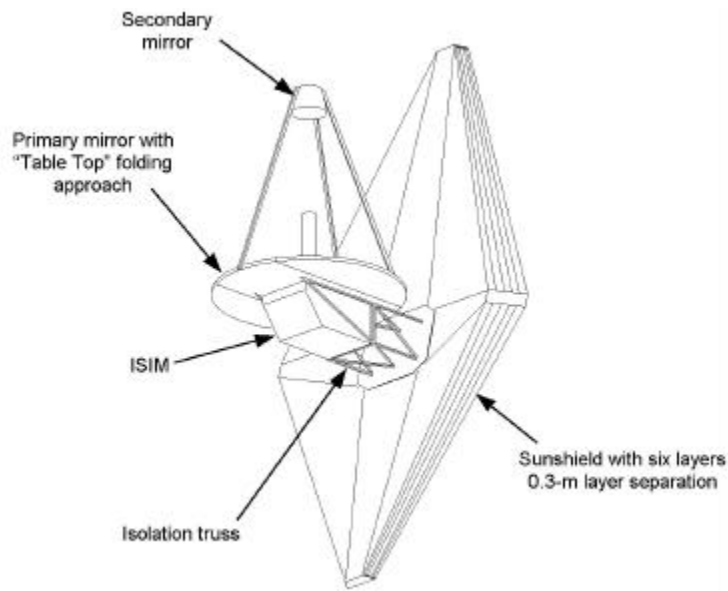


Figure 14. MIR-compatible architecture

Table 5. Thermal data for the MIR-compatible architecture

	0° pointing	27° pointing	DT during slew
Number of sunshield layers	6		
Sunshield effective emissivity	0.0001		
Sunshield temperature (K)	90	87.3	-3.7
Primary mirror temperature			
Average (K)	30.5	29.6	-0.9
Aft petal (K)	26.3	25.5	-0.8
Leading petal (K)	34.7	33.7	-1.0
Petal ΔT (K)	8.4	8.2	-0.2
Power needed to isothermalize (W)	0.082	0.074	
Power needed to maintain temperature stability (W)		0.019	

4.4 MIR-optimized architecture

This scheme (Figure 15) is similar to the previous one, but with a much more effective sunshield. The temperature of the back of the sunshield must be less than about 40 K in order for the heat coming from the sunshield and scattering off the primary and secondary mirrors, to be below the zodiacal light level up to 30 μm (Figure 4). With such an efficient sunshield, the temperature of the OTA/ISIM would naturally be at about 15 K (Figure 3). It is difficult to test large pieces of hardware at such a low temperature and it is very hard to estimate the degradation of key components due to aging when they are used at temperatures so much lower than the general experience base. Since the emission from the primary mirror does not exceed the sunshield emission until the OTA temperature exceeds 40 K there is no need for such a low OTA temperature. Thus, for this option, we have assumed that the OTA/ISIM would be heated to about the same temperature as the MIR-compatible architecture described in section 4.3, or about 40 K.

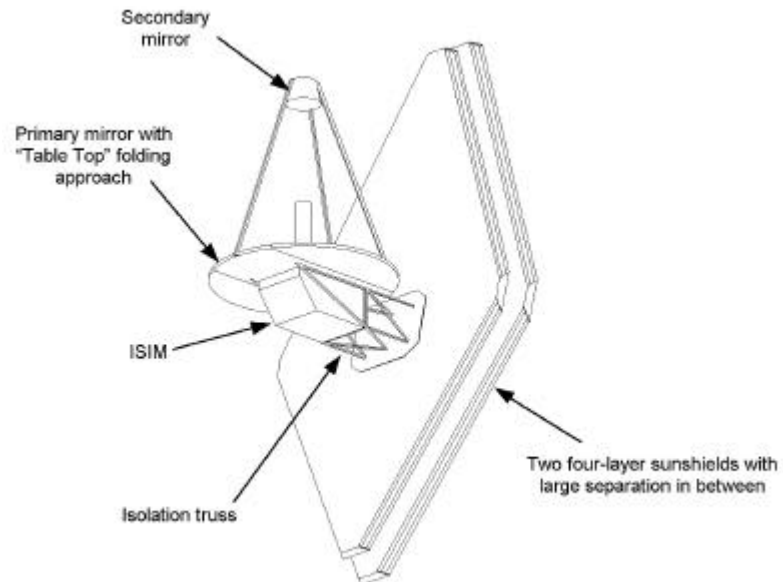
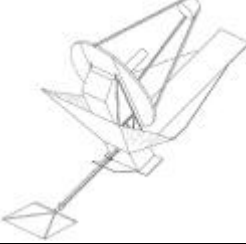
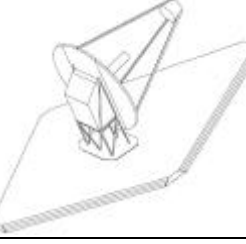
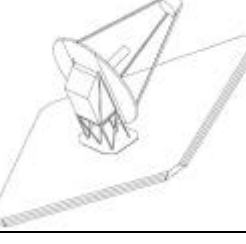
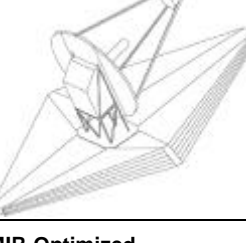
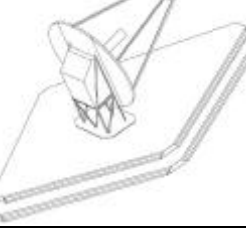


Figure 15. MIR-optimized architecture

5. Cost differences

For cost accounting purposes we calculate cost differences with respect to the NIR-optimized architecture. As described in the sections that follow, these estimates include the differences due to hardware, additional analyses, development efforts, labor increase due to schedule increases, and thermal-vacuum facility modifications to allow using LHe cooling to sub-100 K temperatures. Contingency is added at the rate of 25% generally, and 50% in the case of higher risk items such as the mechanical cryo-cooler and MIR-optimized thermal control elements.

Table 6. Overview of NIR and MIR reference architectures

Architecture	Zodi-limited wavelength	Temperatures	OTA/ISIM Thermal Control	Detector Cooling
NIR-1 	5 μ	Sunshield: 140 K OTA: 100 K ISIM: 90 K	Precision active thermal control	Mechanical cryo-cooler
NIR-2 	5 μ	Sunshield: 140 K OTA: 100 K ISIM: 90 K	Precision active thermal control	Mechanical cryo-cooler
NIR-3 	7 μ	Sunshield: 115 K OTA: 100 K ISIM: 90 K	Large- Δ T open-loop thermal control	Mechanical cryo-cooler
MIR-Compatible 	12 μ	Sunshield: 90 K OTA: 35 K ISIM: 30 K	Small- Δ T open-loop thermal control	NIR: Passive radiative cooling MIR: Solid H ₂ cryostat or mechanical cryo-cooler
MIR-Optimized 	28 μ	Sunshield: 40 K OTA: 35 K ISIM: 30 K	Small- Δ T open-loop thermal control	NIR: Passive radiative cooling MIR: Solid H ₂ cryostat or mechanical cryo-cooler

5.1 Cost of upgrading facilities for using LHe cryogen

Because the cost of adding LHe cooling capability to thermal-vac test chambers is the largest cost difference for adding MIR capability, other than the MIR instrument itself, these costs are broken out separately. The facilities assumed here are based on those specified in a Lockheed Martin preliminary plan for NGST verification and I&T [11]. In Table 7 the required thermal-vac facilities and the needed cryogenes are listed. While separate large thermal-vac facilities are assumed for both the optics and integration contractors, it may be possible to utilize a single large shared thermal-vac facility.

The cost estimates for upgrading these facilities to LHe cooling are presented in Table 8. We have not been able to find a facility that already has the size and the vibration isolation for NGST testing and is currently LHe equipped. The cost estimates for upgrading thermal-vac facilities to LHe capability are based on estimates for GSFC's facility 290 chamber, MSFC's XRCF chamber modifications for NMSD mirror testing, MSFC's estimate for a new large thermal-vac facility to support NGST, and discussions with our potential prime contracting teams. We use an average estimate of \$12M dollars based on all of these sources. Medium and large chamber costs include recycling LHe cryo-coolers. Each small chamber will cost about \$100,000 to upgrade.

Table 9 provides the additional labor costs that result from the longer cool-down and warm-up times required for LHe. For example, in a SIRTf test chamber the cool-down time from ambient to LN2 was about 20 hours and the cool-down time from LN2 to LHe required an additional 4 hours. The time increase for the small cryostats is negligible.

The cost of upgrading the thermal-vac from LN2 to LHe, is estimated to be about \$19M. The major uncertainty is whether the final system test needs to be at low temperature (40 K).

5.2 SSM cost difference estimate

Being on the sun-side of the sunshield, the spacecraft support module is unchanged whether MIR capability is provided or not. The components most affected are the sunshield and thermal isolation truss, with smaller changes occurring in the structure, harness, and electrical power subsystem. The estimated cost differences in the SSM are detailed in Tables 10 and 11 and further discussed below. The total cost of MIR compatibility for the SSM is roughly \$3M.

Sunshield: The baseline sunshield design for an NIR-optimized design consists of four-layers with a layer-to-layer spacing sufficiently small that no additional mechanisms are required to increase the separations after deployment. For the MIR-compatible design, a sunshield with six layers, spaced 0.3 m apart, reaches the required temperatures. This separation is obtained with the addition of a simple spreader mechanism to the tip of each of the four booms. The temperatures required for the MIR-optimized design are reached by using two four-layer sunshields with a large separation between them. Although the two sunshields differ slightly in size, this approach minimizes non-recurring effort and testing

Isolation truss: Since the 100 K OTA of the baseline NIR-optimized design allows relatively high conductive heat loads, the isolation truss can be made from titanium. For the MIR-compatible and MIR-optimized designs we have assumed that gamma-alumina is required in

Table 7. Requirements for thermal testing facilities.

Thermal-vac facility size & location	Test	Cryogen	
		NIR-Optimized	MIR-Compatible & MIR-Optimized
Small cryostat at FSM contractor	Component development testing (phase A/B) and functional testing (phase C/D)	LN2	LHe
Small cryostat at DM contractor	Component development testing (phase A/B) and functional testing (phase C/D)	LN2	LHe
Small cryostat at mirror actuator contractor	Component development testing (phase A/B) and functional testing (phase C/D)	LN2	LHe
Small cryostat at isolation truss contractor	Component development testing (phase A/B) and functional testing (phase C/D)	LN2	LHe
Small Chamber at NIR camera contractor	Testing of NIR camera	LN2	LHe
Small Chamber at NIR spectrograph contractor	Testing of NIR spectrograph	LN2	LHe
Medium chamber at optics contractor	Cryo-figuring of PM segments, SM, and TM; verification of SM and TM	LN2	LHe
Large chamber at optics contractor	PM verification and OTA verification	LN2	LN2
Medium chamber at ISIM integration contractor	ISIM/isolation truss thermal balance	LN2	LHe
Large chamber at systems integration contractor	SSM/Isolation truss thermal balance, sunshield scale model test, and OTA/ISIM thermal balance	LN2	Lhe

Table 8. Estimated cost of upgrading thermal-vac facilities to use LHe cryogen

Chamber size	Quantity	Modification cost each (FY1996\$M)	Total modification cost (FY1996\$M)
Small Cryostat	One each at FSM, DM, mirror actuator, & isolation truss contractors = 4 total	0.05	0.2
Small Thermal-vac	One each at Instrument contractors =2 total	0.2	0.4
Medium Thermal-vac	One at optics contractor, One at ISIM integrator	3.0	6.0
Large Thermal-vac	One at systems contractor	12.0	12.0
Total thermal-vac facilities LHe upgrade cost			18.6

Table 9. Estimated additional labor cost associated with the increased cool-down and warm-up time required to achieve LHe temperatures

Chamber	Extra time per ambient-cold-ambient cycle	Number of cycles	Number of people	Total labor	Labor cost (\$M) @ \$225K/MY
Small chambers at component contractors	1 shift	4 cycles for each instrument = 8 total	6	48 MD = 0.20 MY	0.05
Medium chamber at optics contractor	2 shifts	3 cycles each for 9 primary mirror segments, secondary mirror, & tertiary mirror = 27 total	8	528 MD = 2.20 MY	0.50
Large chamber at optics contractor	4 shifts	2 cycles each for PM verification and OTA verification = 4 total	30	480 MD = 2.0 MY	0.45
Total additional labor cost for increased cool-down/warm-up time for LHe cryogen					1.0

place of titanium. Use of Gamma-alumina requires additional development testing in phase A/B and additional flight hardware costs in phase C/D. For the MIR-optimized architecture, the isolation truss is longer and supports an additional sunshade.

As discussed in section 5.1, one hundred \$100,000 are required for a thermal vac chamber LHe upgrade for testing the isolation truss. Labor costs associated with the longer cool-down/warm-up cycle times for LHe is estimated at \$15,000. These costs are added in phase C/D.

SSM Structure: Adding the MIR instrument and additional sunshield hardware increases the mass that the SSM structure must support during launch. The additional cost for the SSM structure is scaled proportionally to total launch mass. A similar additional increase in effort is required for providing even better thermal isolation in the MIR-optimized design.

SSM thermal control: The increased thermal isolation from the sun and warm SSM required for the MIR-compatible designs require additional thermal control in the vicinity of the SSM and sunshield. It is estimated that this will require three extra man-months of analysis, along with MLI blanket design, fabrication, and installation.

Electrical harness: We have assumed that the MIR-compatible and MIR-optimized designs would require higher cost electrical wiring with an improved ratio of electrical-to-thermal conductivity.

Electrical power subsystem: The lower temperatures of the OTA in the MIR-compatible and MIR-optimized designs require less electrical heater power for thermal control, but additional power for the MIR instrument electronics. It is assumed that these two power changes balance out and that no change is required in the electrical power subsystem..

Table 10. Estimated SSM cost increase for upgrading from an NIR-optimized to an MIR-compatible design

Component or Activity	Delta Cost Estimate	Cost Increase by Project Phase (FY1996\$M)				Cost Increase with Contingency (FY1996\$M)			
		Phase A/B	Phase C/D	Ops Phase	Total	Phase A/B	Phase C/D	Ops Phase	Total
Isolation truss	Engineering estimate of using gamma-alumina material in place of titanium:	0.10			0.10	0.13			0.13
	Gamma-alumina material characterization		0.50		0.50		0.63		0.63
	Increased cost of truss design & fabrication	0.04	0.01		0.05	0.05	0.01		0.06
	Cryostat upgrade to LHe & LHe cryogen costs								
Structure	Asume structure cost increase directly proportional to increase in observatory structure mass of 2% due to addition of MIR: 0.02 x \$10M = \$0.2.		0.20		0.20		0.25		0.25
Thermal control	Engineering estimate of increased analyses & improved insulation around sunshield		0.05		0.05		0.06		0.06
Harness	Estimate cost increase of using more exotic & higher cost wiring at 5% of total harness cost of \$3.2M.		0.16		0.16		0.20		0.20
Sunshield	Engineering estimate of cost increase from adding two film layers and boom-tip layer separation mechanisms.	0.70	0.80		1.50	0.88	1.00		1.88
	ISIM Subtotal	0.84	1.72		2.56	1.05	2.15		3.20

Table 11. Estimated SSM cost increase for upgrading from an MIR-compatible to an MIR-optimized design

Component or Activity	Delta Cost Estimate	Cost Increase by Project Phase (1996\$M)				Cost Increase with Contingency (FY1996\$M)			
		Phase A/B	Phase C/D	Ops Phase	Total	Phase A/B	Phase C/D	Ops Phase	Total
Isolation Truss	Engineering estimate of increased cost of lengthened truss to support two sunshields		0.10		0.10		0.13		0.13
Thermal control	Engineering estimate of increased analyses & improved insulation around sunshield		0.05		0.05		0.06		0.06
Sunshield	Sunshield test flight in GEO or high fidelity sunshield testing and model correlation	5.00			5.00	7.50			7.50
	Engineering estimate of cost difference between one six-layer sunshield and two four-layer sunshields		3.00		3.00		4.50		4.50
SSM Subtotal		5.00	3.15		8.15	7.50	4.69		12.19

5.3 OTA cost difference estimate

The main optical telescope assembly cost differences for the MIR-compatible and MIR-optimized designs are the costs associated with LHe testing mirror elements, fast steering mirror (FSM), deployable mirror (DM), and actuator development testing, and actuator material characterization. The largest costs associated with cryo-temperature testing is the cost of adding LHe-cooled shrouds and LHe recycling coolers or LHe cryogen for smaller chambers, to these thermal-vacuum test facilities. The estimated cost differences in the OTA are detailed in Table 12 and further discussed below. For the MIR-optimized architecture the OTA has been assumed to be the same as the NIR-optimized MIR-compatible architecture. The total OTA cost difference to be MIR compatible, which includes LHe testing and assumes passive cooling to NIR detectors, is approximately \$18M.

Primary, secondary & tertiary mirrors and structure: There is no significant cost difference, other than in the thermal-vac facilities, for the development of the OTA mirrors (DM and FSM not included) and structure. (One should take into account the money already spent in directing the technology toward 40 K instead of 100 K. But, this is not a substantial cost and can be corrected in the Advanced Mirror System Demonstrator procurement.) The OTA mirrors and structure must be “tuned” for the environment in which they will operate. This requires the selection of materials with the proper coefficient of thermal expansion. The analysis effort associated with this selection is essentially the same whether at 40 K or 100 K. Only where properties for new primary mirror materials are lacking at LHe temperatures will there be additional costs for materials testing.

For production of flight mirrors, there is the added cost of upgrading thermal-vac test chambers to LHe temperatures. It is assumed that one medium-size chamber will need to be upgraded for mirror cryo-figuring and secondary and tertiary mirror verification. Medium-size chamber upgrade and additional labor costs are estimated at \$3M and \$410,000 respectively. Additionally, one large chamber will need to be upgraded for final system verification. Large-size chamber upgrade and additional labor costs are estimated at \$12M and \$450,000 respectively.

Table 12. *Estimated OTA cost increase for upgrading from an NIR-optimized to an MIR-compatible design*

Component or Activity	Delta Cost Estimate Basis of Estimate	Cost Increase by Project Phase (FY1996\$M)				Cost Increase with Contingency (FY1996\$M)			
		Phase A/B	Phase C/D	Ops Phase	Total	Phase A/B	Phase C/D	Ops Phase	Total
Primary Mirror	Cost increase for additional properties testing and analysis in developmental phase at LHe temperatures.	0.10			0.10	0.13			0.13
Mirror element test chamber upgrade	Medium-size thermal-vac chamber upgrade to LHe cryogen & associated increased labor costs		3.50		3.50		4.38		4.38
OTA Structure	Cost increase for additional properties testing and analysis in developmental phase at LHe temperatures.	0.10			0.10	0.13			0.13
Deformable Mirror	Additional materials development cost for LHe temperature operation Cryostat upgrade to LHe & LHe cryogen costs	0.30	0.20		0.50	0.38	0.25		0.63
		0.04	0.01		0.05	0.05	0.01		0.06
Fast Steering Mirror	Cryostat upgrade to LHe & LHe cryogen costs	0.04	0.01		0.05	0.05	0.01		0.06
Mirror actuators	Estimated cost increase for extending existing actuator material data base to LHe temperatures. Cryostat upgrade to LHe & LHe cryogen costs	0.20	0.10		0.30	0.25	0.13		0.38
		0.04	0.01		0.05	0.05	0.01		0.06
Thermal Control System	Estimated maximum cost increase for low-temperature thermal control hardware	0.25	0.25		0.50	0.31	0.31		0.63
OTA system verification, I&T	Large thermal-vac chamber upgrade to LHe & associated increased labor costs		12.45		12.45		15.56		15.56
OTA Subtotal		1.07	16.53		17.60	1.34	20.66		22.00

Table 13. *Estimated ISIM cost difference for both the MIR-compatible and MIR-optimized architectures relative to that of the NIR-optimized architecture (MIR instrument cost not included).*

Component or Activity	Delta Cost Estimate Basis of Estimate	Cost Increase by Project Phase (FY1996\$M)				Cost Increase with Contingency (FY1996\$M)			
		Phase A/B	Phase C/D	Ops Phase	Total	Phase A/B	Phase C/D	Ops Phase	Total
Cryo-cooler	Cost savings due to elimination of mechanical cryo-cooler	-1.00	-8.00		-9.00	-1.50	-12.00		-13.50
ISIM test chamber upgrade	Medium-size thermal-vac chamber upgrade to LHe cryogen & associated increased labor costs		3.50		3.50		4.38		4.38
Thermal control	Additional cost of passive radiators and associated thermal analyses	0.10	0.10		0.20	0.13	0.13		0.25
ISIM Subtotal		-0.90	-4.40		-5.30	-1.38	-7.50		-8.88

Deformable mirror: There is a good database of material properties in the 120 K regime. Adding MIR capability requires additional materials research to find the proper materials for sub-100 K operation. The cost of this capability (estimated by one deformable mirror supplier, Xinetics) has been estimated to be possibly as high as \$500,000. To this has been added \$100,000 for upgrading a small thermal-vac chamber to LHe cryogen and \$15,000 for additional associated labor costs.

Fast steering mirror (FSM): Voice coil actuators are used in the FSM. They function essentially independent of temperature. The only cost difference is in the increased testing cost at LHe temperatures. One small thermal-vac chamber will be required. Small-size thermal-vac chamber upgrades to LHe temperatures and additional labor costs are estimated at one hundred \$100,000 and \$15,000 respectively.

Mirror actuators: As for the DM, there is a lack of materials data for sub-100 K operation. An estimated \$300,000 are required in addition to the materials characterization work performed under the DM development effort. The small-size thermal-vac chamber upgrade to liquid helium compatibility, along with the estimate additional labor costs are one hundred \$100,000 and \$15,000 respectively. Should an electromagnetic actuator be used, then no additional material development cost is required.

OTA Thermal control hardware: Since increased precision in heater power is needed for thermal control at approximately 40 K temperatures, an additional \$500,000 are allocated for thermal control hardware and testing.

5.4 ISIM cost difference estimate

The NIR-optimized architecture is the only architecture that absolutely requires a mechanical cryo-cooler. The recurring cost of this cooler is estimated at approximately \$9M not including the substantial development cost, which is assumed to be mostly funded by the Defense Department. In the MIR-compatible architecture, passive cooling is used for both the optical systems and the NIR detectors, thereby saving the cost of a mechanical cryo-cooler. Thus, the cost differences provided in Table 13 below show a cost savings to the ISIM for the MIR-compatible and MIR-optimized architectures. The cost of the MIR instrument is provided in Section 5.6

5.5 System-level thermal control cost difference estimate

Cost increases in the thermal control subsystem for reducing the OTA temperature below 100 K are primarily due to additional thermal analyses and thermal model verification testing. Differences in the costs of thermal subsystem hardware are thought to be insignificant. The estimated cost differences in the system-level thermal control issues are detailed in Table 14 and further discussed below. The cost analysis of the thermal system for the extremely cold MIR-optimized architecture is difficult.

Thermal Analysis: Accurate thermal analyses of cryogenic systems require highly detailed computer models that must accurately simulate all heat flows to and from the cooled item. For NGST, when the size and complexity of the OTA is combined with a desired operating temperature of 40 K or below, the resulting system has numerous radiative and conductive heat paths that are extremely sensitive to analytical error. The total thermal energy of the OTA system (proportional to the fourth power of the absolute temperature) is approximately forty times less at 40 K than at the higher 100 K temperature. An analysis of an OTA at 40 K is much more

Table 14. Estimated system-level thermal control cost increase for upgrading from an NIR-optimized to an MIR-compatible design

Component or Activity	Delta Cost Estimate Basis of Estimate	Cost Increase by Project Phase (FY1996\$M)				Cost Increase with Contingency (FY1996\$M)			
		Phase A/B	Phase C/D	Ops Phase	Total	Phase A/B	Phase C/D	Ops Phase	Total
System-level activities	Additional thermal analyses: parametrics, heat maps, bookkeeping, run times, & energy balances	0.12	0.28		0.40	0.15	0.35		0.50
	More complex thermal model verification: scale model sunshield test, interface tests & characterizations, additional test planning and analyses, and additional ISIM testing	0.48	0.72		1.20	0.60	0.90		1.50
	Thermal hardware: Additional materials & coatings characterization	0.10			0.10	0.13			0.13
System-Level Thermal Subtotal		0.70	1.00		1.70	0.88	1.25		2.13

Table 15 Estimated system-level thermal control cost increase for upgrading from an MIR-compatible to an MIR-optimized design

Component or Activity	Delta Cost Estimate Basis of Estimate	Cost Increase by Project Phase (1996\$M)				Cost Increase with Contingency (FY1996\$M)			
		Phase A/B	Phase C/D	Ops Phase	Total	Phase A/B	Phase C/D	Ops Phase	Total
System-level activities	Estimated cost of increased analyses required for achieving very low sunshield temperature.	0.20	0.30		0.50	0.30	0.45		0.75

sensitive to modeling errors than an analysis of a 100 K OTA because of this large thermal energy difference. Figure 16 illustrates that at 40 K the OTA heat balance would have to be known to within 435 mW to predict the temperature of the OTA to within a 5 K range. At 100 K, the heat balance could be off by 3.8 W and still provide the same 5 K range. This results in additional analysis time due to the detailed bookkeeping that must take place to accurately account for and understand all heat flows within the system. Additional time would also be required to build more detail into the computer models in sensitive areas.

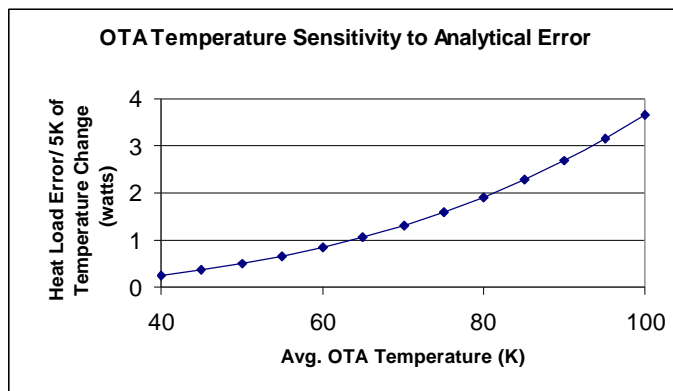


Figure 16. OTA temperature sensitivity to analytical error

At 40 K, thermal model temperature predictions cannot be used to ascertain design margin. Thermal design margin must be determined from the amount of heat flowing into and out of the system. Creating detailed heat maps of the OTA system is time intensive. A 100 K OTA requires less heat mapping due to its relative insensitivity to parasitic heat sources.

Additional analysis time for a 40 K OTA system is also required to analyze the system's sensitivity to various model parameters. These parametric analyses have to be performed with a variety of modeling parameters, such as optical and material properties, interface conductances, etc., to determine where significant sensitivities exist. When such a parameter is identified, then proper design and configuration control have to be implemented to reduce the variance on the parameter. Since a 100 K OTA is less sensitive to parameter variance, fewer parametric thermal analyses need to be performed.

Based on the size and complexity of NGST, we have estimated the extra time needed to thermally analyze a 40 K OTA at two man-years.

Thermal Model Verification: Added modeling complexity requires additional thermal testing to validate the thermal models. Such tests measure material and optical properties to 40 K, characterize the thermal performance of key mechanical interfaces, and verify thermal performance of critical NGST components. Since the MIR-compatible and MIR-optimized architectures incorporate a large high performance sunshield that cannot be thermally tested on the ground, scale model testing will likely be required. The 100 K test temperature required for the NIR-optimized design is not uncommon and there is more confidence and flight history available. A 100 K design requires less thermal testing and relies more on analytical design margin. Since analyses are required to understand the gathered test data, additional analysis costs are incurred due to the additional testing. While some thermal testing is necessary for a 100 K OTA, it is estimated that approximately an additional \$1.2M in test and analysis costs is required for a 40 K OTA.

Thermal Hardware: There is little additional hardware cost penalty for operating the OTA at 40 K versus 100 K. Regardless of temperature, the OTA requires a large sunshield, some type of heater system, insulation, thermal control coatings, temperature sensors, etc. Additional costs could be incurred if the heater system must provide very accurate and stable temperature control instead of the typical coarse temperature control with survival heaters for mechanisms and selected OTA areas. However, even at 100 K, such a type of active heating thermal control might be needed. Regardless of temperature, such a system would require precision heater power supplies and control electronics and highly calibrated temperature sensors.

If the OTA is run at 40 K to provide passive thermal control for the instrument, additional cost is incurred in developing and testing the required instrument radiators. In this case, it is estimated that \$300,000 are needed to purchase the additional hardware for a 40 K OTA.

5.6 MIR instrument cost estimate

Table 16 provides the estimated cost of the MIR instrument and associated instrument accommodation and operation costs. The MIR instrument cost estimate is based on the latest the Yardstick ISIM design [13]. In both the MIR-compatible and the MIR-optimized architectures, the addition of the MIR instrument requires cooling the Si:As detectors to 7 K. For the purpose

of this estimate, we assume the use of a solid-hydrogen cryostat at a cost of \$10M. Operations cost increases for adding MIR capability include additional ground and flight software development and additional operational activities after launch. The largest of these is the flight operations cost, estimated at 15% of the \$300M currently budgeted for flight operations over 10 years.

Table 16. Estimated MIR instrument and associated accommodation and operations costs.

Component or Activity	Delta Cost Estimate Basis of Estimate	Cost Increase by Project Phase (FY1996\$M)				Cost Increase with Contingency (FY1996\$M)			
		Phase A/B	Phase C/D	Ops Phase	Total	Phase A/B	Phase C/D	Ops Phase	Total
ISIM Costs									
Solid cryogen cooler	Cost of solid H2 cooler for MIR detectors	1.00	9.00		1	1.25	11.25		12.50
MIR Instrument	Estimated MIR instrument cost	3.00	24.90		27.90	3.75	31.13		34.88
ISIM common systems	Estimated cost increase to accommodate MIR instrument	0.90	5.40		6.30	1.13	6.75		7.88
ISIM Subtotal		4.90	39.30		44.20	6.13	49.13		55.25
Operations Costs									
S/W development	Engineering estimate of flight S/W design & case test effort increase is 10%, & ground S/W development is 20%. Skill ratio is 75% Sr & 25% Jr level.	1.27	5.06		6.33	1.59	6.33		7.91
Flight ops	Engineering estimate of flight ops & data processing cost for MIR instrument is an additional 15% of total budgeted annual cost of \$300M. $0.15 \times \$40M = \$45M$			45.00	45.00			45.00	45.00
Operations Subtotal		1.27	5.06	45.00	51.33	1.59	6.33	45.00	52.91
Total estimated cost of adding MIR instrument		6.17	44.36	45.00	95.53	7.72	55.46	45.00	108.16

5.7 Cost summary

Table 17 provides the top-level summary of the cost differences analyzed above. The estimated phase C/D cost differences of the MIR-compatible and MIR-optimized options over that of the NIR-optimized architecture are \$16.6M and \$21.7M respectively, including contingency. Based on a \$400M budget for phase C/D, these costs represent 4.2% and 5.4% respectively.

When the MIR instrument and associated accommodation and operations costs are included, the total additional phase C/D/E costs are \$117M and \$122M, respectively, which represents increases of approximately 13% to the budgeted \$900M.

Table 17. Summary cost difference for adding MIR capability

Cost element	Cost Increase with Contingency Relative to NIR-Optimized Architecture (FY1996\$M)							
	MIR-Compatible Option				MIR-Optimized Option			
	Phase A/B	Phase C/D	Ops Phase	Total	Phase A/B	Phase C/D	Ops Phase	Total
NIR instrument only								
SSM	1.05	2.15	---	3.20	8.55	6.84	---	15.39
OTA	1.34	20.66	---	22.00	1.34	20.66	---	22.00
ISIM	-1.38	-7.50	---	-8.88	-1.38	-7.50	---	-8.88
Thermal (system level)	0.88	1.25	---	2.13	1.18	1.70	---	2.88
Total increase for MIR compatibility w/o MIR instrument	1.89	16.56	---	18.45	9.69	21.70	---	31.39
NIR + MIR instruments								
SSM	1.05	2.15	---	3.20	8.55	6.84	---	15.39
OTA	1.34	20.66	---	22.00	1.34	20.66	---	22.00
ISIM	4.75	41.63		46.37	4.75	41.63		46.37
Thermal (system level)	0.88	1.25	---	2.13	1.18	1.70	---	2.88
Operations	1.59	6.33	45.00	52.91	1.59	6.33	45.00	52.91
Total increase including MIR instrument	9.61	72.02	45.00	126.61	17.41	77.16	45.00	139.55

6. Discussion

Figure 17 illustrates how the total cost for the observatory varies with wavelength coverage. For this purpose of showing cost differences with respect to absolute cost, we have anchored the MIR-compatible option at \$400M. It is important to note that the MIR-compatible option falls in a local minimum. This is because the sunshield is efficient enough to passively cool the detectors and eliminate the need for a mechanical cryo-cooler, while avoiding the development and test costs associated with a very cold sunshield.

It is the test facility upgrades that makes the MIR-compatible architecture more costly than in the NIR-optimized architecture. However, it should be noted that we have used the worst case scenario by assuming that the MIR-compatible architecture need LHe testing while assuming the NIR-optimized system will need LN2 testing. In fact, it may very well be that both architectures need large a LHe thermal-vac chamber to do realistic thermal tests.

While the costs of the three architectures considered are similar (~5%), the risks are quite different. The NIR-optimized design requires a cryo-cooler that has not yet been developed and is thus a higher risk element. No existing cryo-cooler meets the NGST requirements and accelerated life testing of the cryo-cooler is not possible and that risk will be carried well into phase C/D. In contrast, the risk associated with the efficient sunshield used in the MIR-compatible architecture can be retired in phase B. Indeed, there is a clear strategy to add robustness to this design by a two tier approach. First, extensive ground and space testing of the

sunshield will be performed to reduce design uncertainty. Second, the sunshield can be “over-designed” by including extra layers of sunshield that increases the overall margin at low cost. Extending this technology to the MIR-optimized architecture greatly increases the risk because of the extremely low temperature sunshield. The required performance of the sunshield and knowledge of degradation processes are clearly outside of the current experience base. Moreover, the testing program for this configuration is extremely difficult because of the very low temperatures.

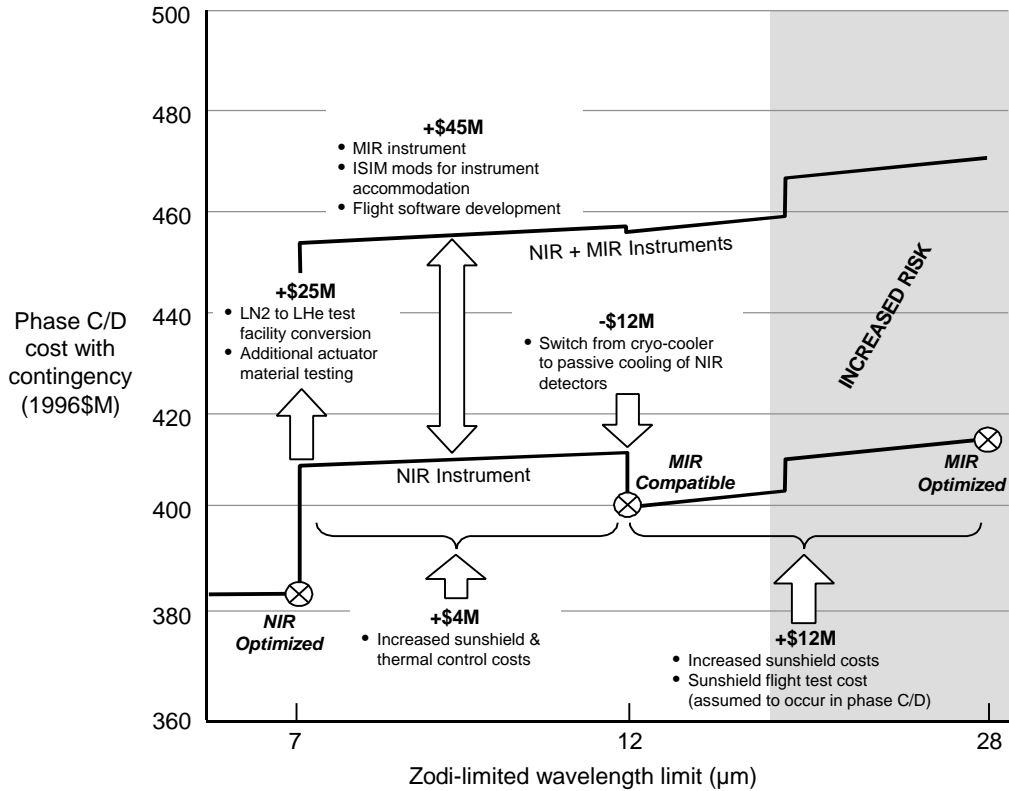


Figure 17 Cost of NGST as a function of infrared wavelength coverage

7. Conclusion

What initially appeared to be a low cost solution for a purely NIR-optimized NGST (NIR1, 2 or 3) is upon closer examination a more complex and riskier solution than those which have been proposed so far for a MIR-compatible observatory. The savings offered by the easier testing on the ground of a NIR-optimized system are offset by the need for precise temperature control of the optics and the cost of the cryo-cooler for the NIR detectors. In the end, a passively cooled observatory appears a more natural technical solution and has the advantage of keeping the option of adding the MIR instrument open (e.g. for international collaborators). We finally note that such a solution is consistent with the main requirements for the Terrestrial Planet Finder (TPF) component of the Origins program and thus adds further to NGST being a logical precursor to the TPF mission.

We therefore recommend that the MIR-compatible configuration remain the baseline for further NGST study.

Acknowledgements

We wish to thank many of our colleagues for contributing to or reviewing this work, in particular Harley Thronson (NASA HQ), Joe Burt, Jon Lawrence, and Dan Blackwood (GSFC); Peter Stockman (STScI); Jim Crocker, Doug Neam, and Bob Woodward (Ball Aerospace); Frank Martin, Mike Menzel, and Greg Anderson (Lockheed-Martin); Greg Davidson, Charles Atkinson, and Ralph Schilling (TRW), Mark Lysek and Tom Luchik (JPL) and Tim Hawarden (Joint Astronomy Center). We would also like to thank John Mather and Bernie Seery for encouraging this work and Edward Weiler (NASA HQ) for his insightful comments.

References

1. *HST and Beyond*, A. Dressler ed., Space Telescope Science Institute, 1996
2. NGST, visiting a time when galaxies were young, H.S. Stockman editor, 1997
3. *The NGST Yardstick Mission*, NGST monograph No 1, 1998 (in preparation).
4. P.Y. Bély, *The NGST "Yardstick Mission"*, In "Science with the NGST", Proc. ESA Workshop, Liege, 1998.
5. TRW Pre-phase A proprietary report, 1998.
6. Ball Aerospace Pre-Phase A proprietary report, 1998.
7. P.Y. Bély, L. Petro, K.I. Mehalick,, C.M. Perrygo, *Straylight analysis of NGST*, SPIE Proc. 3356, 1998.
8. C. M. Perrygo, M. Choi, K. Parrish, R.G. Schunk, D. Stanley, E.M. Wooldridge, *Passive thermal control of the NGST*, SPIE Proc. 3356, 1998.
9. J. Nelson, *Segmented mirror design for a 10-meter telescope*, SPIE Proc. 172, 1979.
10. K. Lau, W. Breckenridge, N. Nerheim, D. Redding, *Active figure maintenance control using an optical laser truss metrology system for a space-based far-IR segmented telescope*, SPIE Proc. 1696, p 60, 1992.
11. M. Menzel, K. Triebes and D. Leary, *A strawman verification, integration and test program for the Next Generation Space Telescope*, LMSC report, 1998.
12. NGST Quarterly, Oct 1997.
13. M. Greenhouse, ISIM NGST Project Office study, 1998.